Cancer Imaging (2013) **13(4),** 557–566
DOI: 10.1102/1470-7330.2013.0049

ORIGINAL ARTICLE

In vivo monitoring of sorafenib therapy effects on experimental prostate carcinomas using dynamic contrast-enhanced MRI and macromolecular contrast media

Clemens C. Cyran[a,1], Bettina Schwarz[b,1], Philipp M. Paprottka[a], Steven Sourbron[c,d], Jobst C. von Einem[a], Olaf Dietrich[c], Rabea Hinkel[e], Dirk A. Clevert[a], Christiane J. Bruns[b], Maximilian F. Reiser[a], Konstantin Nikolaou[a], Bernd J. Wintersperger[a,f]

[a]Department of Clinical Radiology, Laboratory for Experimental Radiology, University of Munich Hospitals – Campus Grosshadern, Ludwig-Maximilians-University Munich, Marchioninistrasse 15, 81377 Munich, Germany; [b]Department of Surgery, University of Munich Hospitals – Campus Grosshadern, Ludwig-Maximilians-University Munich, Marchioninistrasse 15, 81377 Munich, Germany; [c]Josef Lissner Laboratory for Biomedical Imaging, Department of Clinical Radiology, University of Munich Hospitals – Campus Grosshadern, Ludwig-Maximilians-University Munich, Marchioninistrasse 15, 81377 Munich, Germany; [d]Division of Medical Physics, University of Leeds, Leeds, UK; [e]Department of Cardiology, University of Munich Hospitals – Campus Grosshadern, Ludwig-Maximilians-University Munich, Marchioninistrasse 15, 81377 Munich, Germany; [f]Department of Medical Imaging, University Health Network, University of Toronto, 585 University Avenue, Toronto ON M5G 2N2, Canada

Corresponding address: Clemens C. Cyran, Department of Clinical Radiology, Laboratory for Experimental Radiology, University of Munich Hospitals – Campus Grosshadern, Ludwig-Maximilians-University Munich, Marchioninistrasse 15, 81377 Munich, Germany.
Email: clemens.cyran@med.lmu.de

[1]C.C. Cyran and B. Schwarz contributed equally to this research project, and share first authorship.

Date accepted for publication 5 November 2013

Abstract

Purpose: To investigate dynamic contrast-enhanced magnetic resonance imaging (DCE-MRI) with macromolecular contrast media (MMCM) to monitor the effects of the multikinase inhibitor sorafenib on subcutaneous prostate carcinomas in rats with immunohistochemical validation. **Materials and methods:** Copenhagen rats, implanted with prostate carcinoma allografts, were randomized to the treatment group ($n = 8$) or the control group ($n = 8$). DCE-MRI with albumin-$(Gd\text{-}DTPA)_{35}$ was performed at baseline and after 1 week using a clinical 3-Tesla system. The treatment group received sorafenib, 10 mg/kg body weight daily. Kinetic analysis yielded quantitative parameters of tumor endothelial permeability–surface area product (PS; ml/100 ml/min) and fractional blood volume (V_b, %). Tumors were harvested on day 7 for immunohistochemical analysis. **Results:** In sorafenib-treated tumors, PS (0.62 ± 0.20 vs 0.08 ± 0.09 ml/100 ml/min; $P < 0.01$) and V_b (5.1 ± 1.0 vs $0.56 \pm 0.48\%$; $P < 0.01$) decreased significantly from day 0 to day 7. PS showed a highly significant inverse correlation with tumor cell apoptosis (TUNEL; $r = -0.85$, $P < 0.001$). Good, significant correlations of PS were also observed with tumor cell proliferation (Ki-67; $r = 0.67$, $P < 0.01$) and tumor vascularity (RECA-1; $r = 0.72$, $P < 0.01$). MRI-assayed fractional blood volume V_b showed a highly significant correlation with tumor vascularity (RECA-1; $r = 0.87$, $P < 0.001$) and tumor cell proliferation (Ki-67; $r = 0.82$, $P < 0.01$). **Conclusion:** Results of DCE-MRI with MMCM demonstrated good, significant correlations with the immunohistochemically assessed antiangiogenic, antiproliferative, and proapoptotic effects of a 1-week, daily treatment course of sorafenib on experimental prostate carcinoma allografts.

Keywords: *Dynamic contrast-enhanced MRI; drug response biomarker; sorafenib; prostate carcinoma; immunohistochemistry.*

Introduction

Novel molecular therapies targeting various steps of the angiogenic cascade are currently being investigated in oncology, with inhibitors of vascular endothelial growth factor (VEGF) in the forefront[1]. Depending on the class of antiangiogenic agent, endothelial cell proliferation, microvessel formation, and tumor cell growth or survival is primarily affected by the different treatment strategies[2,3]. As a multityrosine kinase inhibitor, sorafenib has been shown to exhibit antiangiogenic, antiproliferative, and proapoptotic effects on a range of different tumor entities, including the investigated experimental model of prostate cancer[4,5]. In the clinical setting, sorafenib has already been approved for the treatment of patients with unresectable hepatocellular carcinoma and advanced renal cell carcinoma[6,7], and a recent phase II clinical trial has investigated sorafenib for treatment of metastatic and castration-resistant prostate cancer, with some success[8,9]. Traditional morphologic assessment of tumor response to therapy, such as tumor size-dependent RECIST (Response Evaluation Criteria in Solid Tumors) criteria, has been shown to be not sensitive enough for the reliable evaluation of tumor response to antiangiogenic therapy[10]. As the mode of action of novel targeted tumor therapies is not primarily cytotoxically associated with tumor shrinkage, but with early effects on tumor microcirculation and metabolism[11], functional imaging methods may be more suitable for the development of noninvasive imaging biomarkers of therapy response. Multiple preclinical studies have investigated perfusion imaging techniques based on magnetic resonance imaging (MRI) and computed tomography (CT) for the detection of functional response of tumors in different forms of angiogenesis-inhibiting therapy, with varying success[12,13]. Most of the performed perfusion studies applied clinically available, small molecular contrast media (SMCM) with an unspecific, extracellular distribution profile for the noninvasive assessment of tissue microcirculation[13,14]. However, preclinical perfusion studies using macromolecular contrast media (MMCM) have demonstrated their potential in the quantification of functional parameters of microcirculation shown to reflect metabolic tumor response to antiangiogenic treatment with high sensitivity[15,16]. This increased sensitivity is attributed to a pronounced extravasation of MMCM molecules in angiogenically active tissues stimulated by VEGF. VEGF is known as a central mediator of angiogenesis and endothelial permeability to small and large molecules[17] where the permeability value p should always be specified for one specific molecule or ion. Availability of a functional imaging method providing insights into the vascular physiology of tumors may allow for a noninvasive and more accurate prediction of therapeutic efficacy and early stratification of responders from nonresponders.

We therefore hypothesized that dynamic contrast-enhanced (DCE)-MRI enhanced with MMCM is able to assess the anti-angiogenic effects of sorafenib on experimental prostate carcinoma with good correlation to immunohistochemistry. The aim of this study was to assess the suitability of MMCM in comparison with SMCM data gathered by our group in previous experiments[5], in the same model of prostate cancer under sorafenib therapy, to evaluate possible advantages of MMCM for monitoring response to antiangiogenic therapy.

Materials and methods

Animal model and experimental protocol

The study was performed with the approval of the Institutional Committee for Animal Research and in accordance with the guidelines of the National Institutes of Health for the care and use of laboratory animals. A total of 16 Copenhagen rats (7–8 weeks old, Harlan Laboratories, Indianapolis, IN) were subcutaneously injected with 6×10^6 rat prostate carcinoma cells MLLB-2 (Mat Ly Lu-B2) into the left abdominal flank. Daily animal inspection was conducted for general appearance and tumor growth. When tumors reached a volume of approximately 800 mm^3 based on caliper measurements in 3 dimensions (tumor volume $mm^3 = a \times b \times c \times 0.5$), animals were randomly assigned to either the therapy group ($n = 8$) or the control group ($n = 8$). Sorafenib (Nexavar; Bayer Schering Healthcare, Leverkusen, Germany) treatment of the therapy group (10 mg/kg body weight) and placebo treatment (volume-equivalent application of the solvent solution cremophor/ethanol only) of the control group via daily gastric gavage followed an established treatment protocol[5]. DCE-MRI was performed prior to therapy initiation (day 0) and on day 7 following therapy. Prior to the MRI examinations, animals were anesthetized by intraperitoneal injections of ketamine (100 mg/kg body weight) and xylazine (10 mg/kg body weight) followed by the insertion of a 25-gauge butterfly tail vein catheter for administration of contrast agent. After completion of the MRI scan at day 7, animals were euthanized by intravenous injection of 1 ml ketamine/xylazine. Tumors were harvested and fixed with formaldehyde (4%) for immunohistochemical analysis.

DCE-MRI

DCE-MRI was performed on a clinical 3-Tesla system (Magnetom Verio; Siemens Healthcare, Erlangen, Germany) with animals in the supine position, using an 8-element phased-array wrist coil for signal reception. Prior to administration of contrast agent, 4 baseline high-resolution data sets were acquired using a three-dimensional (3D) spoiled-gradient echo (GRE) technique (repetition time 9.7 ms; echo time 4.8 ms; $\alpha = 40^\circ$) in axial orientation with an acquisition time of 59.6 s per data set. Using a matrix size of 128×128 and

a field of view (FOV) of $50 \times 50\,mm^2$, a spatial resolution of $0.39 \times 0.39 \times 3.0\,mm^3$ was achieved, with 72 mm of coverage along the *z*-axis. With the initiation of the manual injection of albumin-(Gd-DTPA)$_{35}$, 0.03 mmol/kg body weight (blood half-life 54 ± 11 min) followed by a NaCl bolus, the high-resolution 3D GRE sequence as already applied prior to contrast injection was continued to follow delayed contrast-enhancement characteristics. The number of acquired 3D data sets was 55, resulting in a total time of acquisition of 55 min. Because of the known macromolecular behavior and slow kinetics of albumin-(Gd-DTPA)$_{35}$[18], a low temporal resolution of approximately 1 min was chosen for dynamic data acquisition.

Contrast agent

Albumin-(Gd-DTPA)$_{35}$ was synthesized following a published method[19] and has an actual molecular weight of approximately 92 kDa, but its effective molecular weight resembles that of a 180-kDa globulin, as measured by size-exclusion high-performance liquid chromatography with comparison to protein standards. This prototype MMCM approaches the kinetics of proteins, remains primarily intravascular in physiologic vessels, and is known to extravasate through the hyperpermeable endothelium of pathologic tumor vessels to accumulate in the interstitial compartment. Albumin-(Gd-DTPA)$_{35}$ was applied at a dose of 0.03 mmol Gd per kg body weight by a fast manual bolus injection via the tail vein catheter.

MRI data processing and kinetic analysis

Data were postprocessed on an external workstation using the software PMI 0.4 (Platform for Research in Medical Imaging), written in IDL 6.4 (ITT Visual Information Solutions, Boulder, CO, USA)[20,21]. An arterial region of interest (ROI) was drawn within the lumen of the abdominal aorta, and a tissue ROI was placed over the tumor periphery (Fig. 1). The tumor periphery was defined as the outer 2-mm rim of the tumor excluding the skin. The defined tumor periphery has been shown to be a good representation of viable tumor tissue, less affected by elevated interstitial pressure and necrosis that may occur in the tumor center[22]. To capture predominantly vital tumor tissue, MRI perfusion analysis was performed on a single slice 5 mm away from the cranial or caudal tumor margin in all tumors. The location of MRI perfusion analysis was available when choosing the tumor area for immunohistochemical workup to guarantee an approximated match. Signal–time curves were extracted for both ROIs, and tracer concentrations were approximated by subtracting the baseline signal. Data were fitted to the Patlak model, producing two independent parameters V_b and PS[23]. The fractional blood volume V_b (ml blood per 100 ml tissue) measures the vascularity of the tumor. The endothelial permeability–surface area product PS (ml/100 ml/min) measures the combined effect of the permeability of the capillary wall to albumin-(Gd-DTPA)$_{35}$ (p), and the total surface area of the capillaries in 100 ml tissue (S).

Immunohistochemistry

The effects of sorafenib on the experimental prostate carcinomas were investigated by immunohistochemistry following standard staining procedures for tumor microvascular density (RECA-1), tumor cell proliferation (Ki-67), and tumor cell apoptosis (TUNEL) as previously published[5]. In brief, morphologic tumor tissue analysis was performed by hematoxylin–eosin (H&E) staining, and the necrotic area was measured per high-power field at 100× magnification. Tumor vascularity was assessed as microvascular density (MVD) by RECA-1 staining using a monoclonal mouse antirat antibody against rat endothelial cell antigen as the primary antibody (ab9774, 1:40; Vector Labs, Loerrach, Germany). Slides were incubated at 4°C overnight with subsequent incubation of the secondary antibody (rabbit antimouse secondary antibody, 1:150; Vector Labs) for 1 h at room temperature. For the quantification of MVD, 10 random 0.159-mm^2 fields were captured at 200× magnification for each tumor using an AxioCam camera mounted on

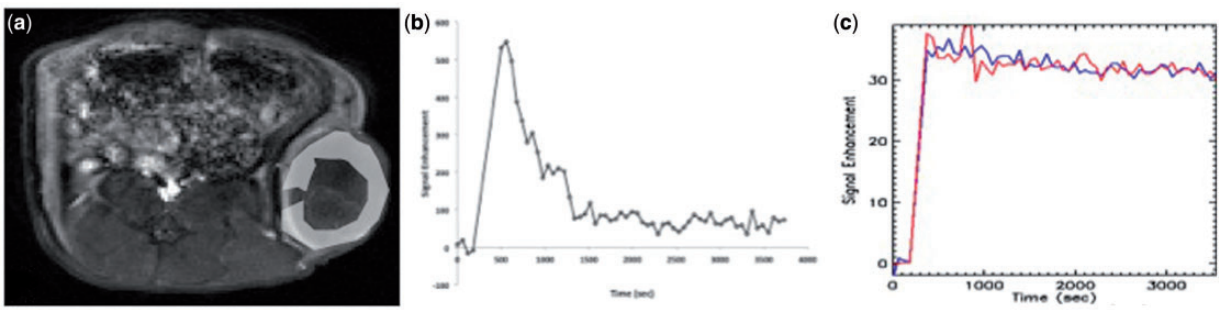

Figure 1 **(a) Donut-shaped region of interest over the subcutaneous prostate carcinoma allograft on an axial T1-weighted, contrast-enhanced magnetic resonance (MR) image. (b) Representative arterial input function. (c) Tumor signal enhancement curve (red) from a baseline examination along with the fit of the Patlak model (blue).**

Carl Zeiss universal microscope and AxioVision software as published previously[24]. Tumor cell proliferation was assessed by Ki-67 antigen staining using a Ki-67-specific monoclonal rabbit antirat antibody (ab16667, 1:100). After application of the primary antibody (ab16667, 1:100; Vector Labs) and overnight incubation at 4°C, the secondary antibody (goat antimouse secondary antibody 1:100; Vector Labs) was applied. Tumor sections were examined microscopically and the average number of Ki-67-positive cells per high-power field was counted at 200× magnification[5]. Tumor cell apoptosis was assessed by staining for TUNEL (terminal deoxynucleotidyl transferase-mediated nick-end labeling) using a commercially available apoptosis detection kit (In Situ Cell Death Detection Kit; Roche Diagnostics, Indianapolis, IN, USA). TUNEL staining was performed according to the manufacturer's instructions (www.roche-applied.science.com). Samples were analyzed under a fluorescence microscope using a standard fluorescent filter set at 520 ± 20 nm. Results were expressed as the average of apoptotic cells in 10 random fields at 200× magnification[5].

Microscopic quantification

Microscopic quantification was performed as previously described in detail[5], using custom-programmed MatLab software (MatLab7 including Image Processing Toolbox; The MathWorks, Natick, MA, USA), parts of which were based on MatLab codes provided by Baris Sumengen (Department of Electrical and Computer Engineering, University of California, Santa Barbara, CA, USA).

Statistical analysis

Continuous variables are presented as mean ± standard deviation. DCE-MRI and immunohistochemistry values between the treatment and the control groups were compared using an unpaired *t*-test. For intragroup comparisons of the DCE-MRI perfusion parameters between day 0 and day 7, a paired *t*-test was applied. Analyses were carried out using SPSS for Windows (version 11.5; IBM, Armonk, NY, USA). Relationships between DCE-MRI and immunohistochemistry were evaluated using Pearson's correlation coefficients. Corrections for multiple comparisons were performed using the Bonferroni method. Values of $P < 0.05$ were considered statistically significant.

Results

Animals tolerated all procedures well, with no adverse effects noted. DCE-MRI and immunohistochemical analysis was successfully performed in all animals.

Tumor volume

In the sorafenib-treated therapy group, tumor volume decreased significantly ($P < 0.05$) over the 1-week, daily treatment course from a mean volume of 4.5 cm^3 at baseline to 3.4 cm^3 at day 7. Tumors of the control group showed a significant increase in tumor volume from an average volume of 4.3 cm^3 at baseline to 14.6 cm^3 on day 7 ($P < 0.05$).

DCE-MRI

The Patlak model fitted the DCE-MRI data well in all studies. A representative set of T1-weighted MR images is shown in Fig. 2. In the sorafenib-treated therapy group, the PS (ml/100 ml/min) decreased significantly ($P < 0.01$) over the course of the experiment from baseline to day 7 (0.62 ± 0.20 vs 0.08 ± 0.09 ml/100 ml/min). No significant change ($P > 0.05$) of PS was observed in the control group treated with cremophor/ethanol between baseline and day 7 (0.45 ± 0.24 vs 0.41 ± 0.12 ml/100 ml/min, $P > 0.05$). Note the unidirectional decline of PS values from baseline to day 7 under sorafenib treatment (Table 1, Fig. 3). Fractional blood volume V_b, as a parameter of tumor vascularity decreased significantly ($P < 0.05$) under sorafenib treatment from day 0 to day 7 ($5.1 \pm 1.0\%$ vs $0.56 \pm 0.48\%$). No significant change in V_b was observed in the control group treated with cremophor/ethanol between baseline and day 7 ($4.4 \pm 1.5\%$ vs $5.3 \pm 2.6\%$, $P > 0.05$). Individual values for both MRI parameters are shown in Table 1.

Immunohistochemistry

H&E staining revealed a significant difference in the amount of vital tumor tissue between the therapy group and the control group (5.9 ± 1.2 vs 9.5 ± 1.1; $P < 0.01$) (Fig. 4A and B). On the one hand, the therapy group demonstrated significantly lower tumor vascularity (RECA-1) than the control group (400 ± 3 vs 1626 ± 32; $P < 0.002$) (Fig. 4C and D). On the other hand, significantly more proliferating cells (Ki-67 staining) were observed in the control group in comparison with the therapy group ($118{,}461 \pm 2311$ vs $65{,}008 \pm 758$, $P < 0.02$) (Fig. 5A and B). Staining for tumor cell apoptosis (TUNEL) revealed significantly fewer apoptotic cells in the control group than in the therapy group ($15{,}262 \pm 418$ vs $35{,}602 \pm 374$, $P < 0.001$) (Fig. 5C and D).

Correlation between DCE-MRI parameters and immunohistochemistry

PS showed a significant inverse correlation with immunohistochemical tumor cell apoptosis (TUNEL; $r = -0.85$, $P < 0.001$). Weaker, but significant correlations of PS were observed with immunohistochemical tumor cell proliferation (Ki-67; $r = 0.67$, $P < 0.01$) and tumor vascularity (RECA-1; $r = 0.72$, $P < 0.01$). MRI-

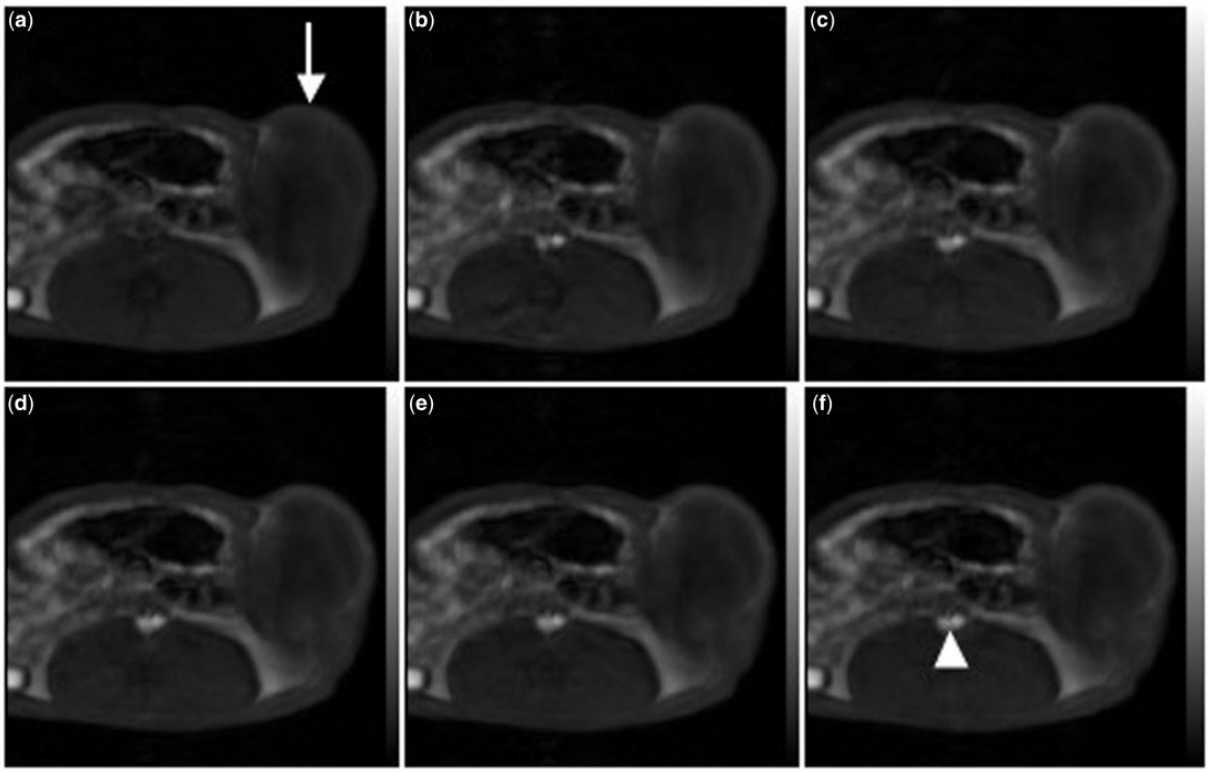

Figure 2 **Representative set of T1-weighted, spoiled-gradient dynamic contrast-enhanced (DCE)-MR images precontrast (a), and at 5 (b), 10 (c), 15 (d), 30 (e), and 60 (f) min after intravenous injection of the macromolecular contrast medium albumin-(Gd-DTPA)$_{35}$ in a baseline therapy animal. White arrow points to the predominantly rim-enhancing pattern of the subcutaneous prostate cancer allograft over the left flank of the rat as well as the prolonged enhancement of the abdominal aorta 60 min post infection (arrowhead).**

Table 1 **Individual values of DCE-MRI parameters of tumor microcirculation, tumor permeability–surface area product (PS), and fractional blood volume (V_b) in the therapy and control groups at baseline and on follow-up scans**

	Animal	PS (ml/100 ml/min)		V_b (%)	
		Day 0	Day 7	Day 0	Day 7
Therapy	1	0.73	0.05	3.9	0.8
	2	0.79	0	5.4	0.4
	3	0.91	0.26	4.5	0
	4	0.64	0.009	5.0	1.2
	5	0.37	0	4.3	0
	6	0.69	0.072	4.4	1.1
	7	0.52	0.11	6.8	0.2
	8	0.34	0.14	6.3	0.8
	Mean	0.62 ± 0.2	0.08 ± 0.09*	5.1 ± 1.0	0.56 ± 0.48*
Control	9	0.88	0.63	4.9	0.8
	10	0.34	0.23	5.6	8.0
	11	0.14	0.32	5.4	5.5
	12	0.56	0.5	5.9	6.0
	13	0.56	0.36	5.1	8.2
	14	0.2	0.42	3.8	2.7
	15	0.35	0.35	2.2	4.5
	16	0.53	0.43	2.1	6.8
	Mean	0.45 ± 0.24	0.41 ± 0.12	4.4 ± 1.5	5.3 ± 2.6

*Significant difference ($P < 0.05$) between day 0 and day 7.

assayed V_b, as a measure of tumor vascularity, showed a highly significant correlation with immunohistochemical tumor vascularity (RECA-1; $r = 0.87$, $P < 0.001$) and tumor cell proliferation (Ki-67; $r = 0.82$, $P < 0.01$). No significant correlation was observed between V_b and tumor cell apoptosis (TUNEL; $r = -0.3$, $P > 0.05$). Individual correlations of quantitative perfusion parameters assessed with MMCM are presented in Table 2 and compared with perfusion parameters evaluated with a conventional SMCM (molecular weight 0.6 kDa) (Table 3), as previously published[5].

Discussion

DCE-MRI

Functional imaging modalities such as DCE-MRI represent a promising approach for monitoring the effects of antiangiogenic therapies in vivo, with the benefit of timely and repeated assessments of therapy response in patients. In preclinical DCE imaging, contrast agents of different molecular weights are available, with a number of studies reporting higher sensitivity of MMCM for the assessment of tissue angiogenic activity[25–27]. DCE-MRI

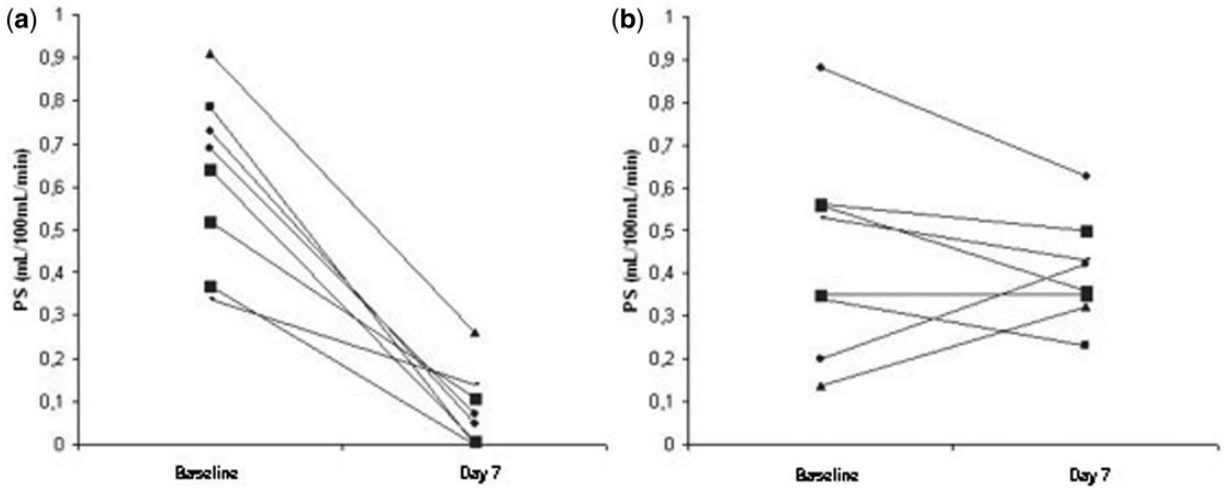

Figure 3 **Line graphs depict the development of the endothelial permeability–surface area product (PS) in the therapy group (left) and the control group (right) from baseline to day 7. Note the unidirectional decline of all PS tumor values between baseline and day 7 under sorafenib treatment.**

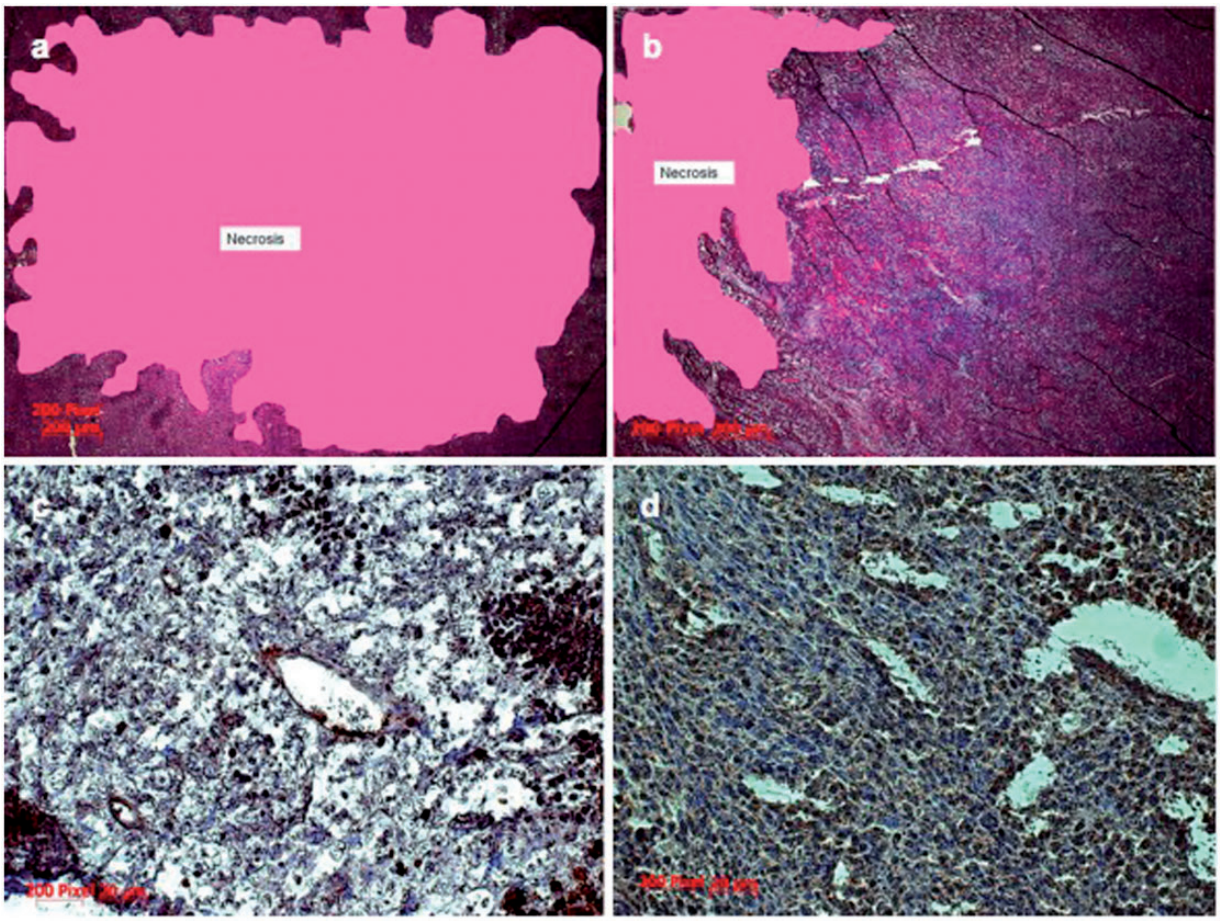

Figure 4 **Hematoxylin–eosin staining of tumor tissue sections highlight larger necrotic areas in a representative tumor section of the therapy group (a) and the control group (b). Representative tumor sections stained for RECA-1 demonstrate significantly fewer endothelial cells stained in brown in the therapy group (c) than in the control group (d).**

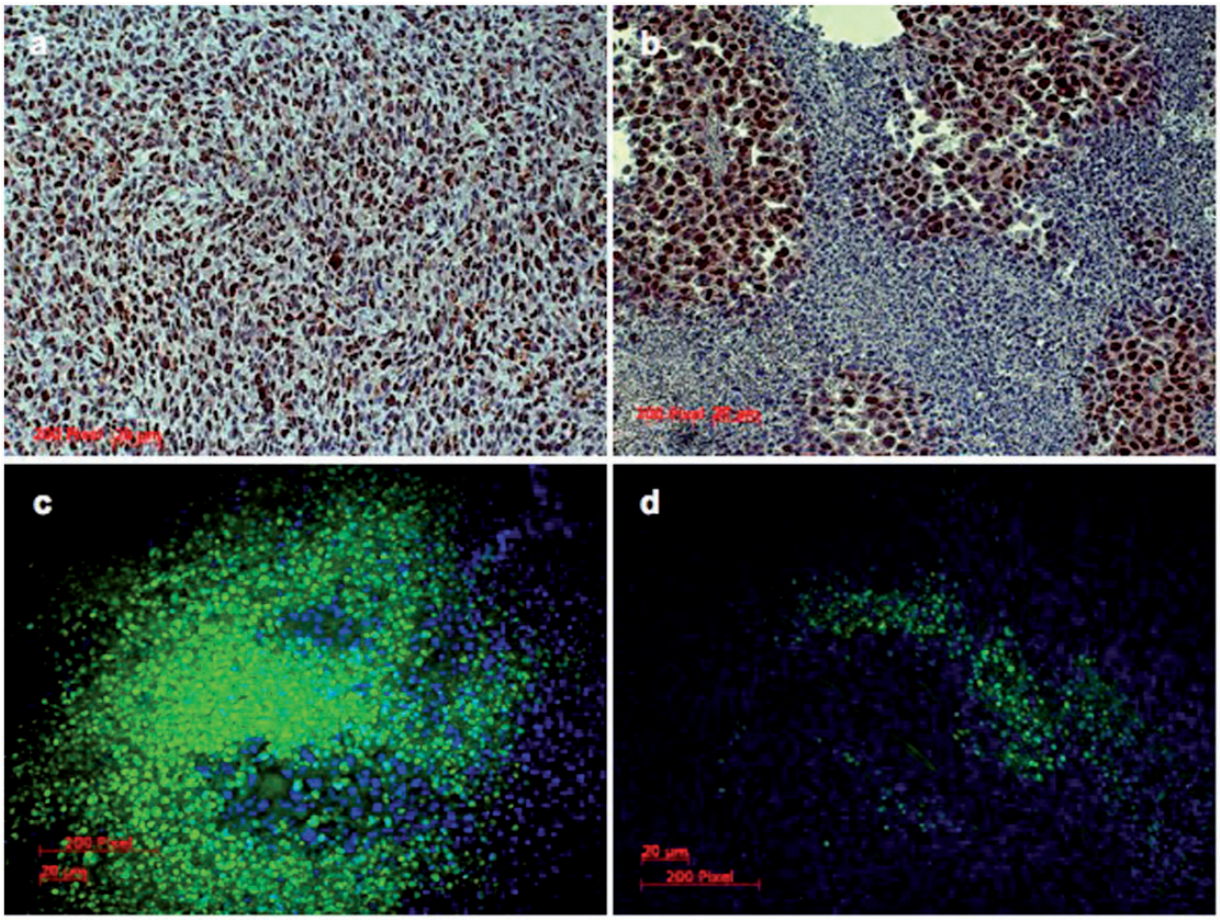

Figure 5 **Tissue section in a representative high-power field (20 ×) from the tumor rim shows a significantly lower amount of proliferating cells (brown nucleus in Ki-67 staining) in the therapy group (a) than in the control group (b). TUNEL staining for apoptosis demonstrates significantly more apoptotic cells (green fluorescence) in the therapy group (c) in comparison with the control group (d).**

Table 2 **Assessment of tumor microcirculation with macromolecular contrast media (MMCM)**

	PS		V_b	
	Correlation (r)	P value	Correlation (r)	P value
RECA-1	0.72	<0.01*	0.87	<0.001*
Ki-67	0.68	<0.01*	0.83	<0.001*
TUNEL	−0.86	<0.001*	−0.3	n.s.

Correlation coefficients (Pearson's r) of noninvasive tumor endothelial permeability (PS) and tumor vascularity (blood volume, V_b) quantified by DCE-MRI and MMCM with immunohistochemical measurements of tumor vascularity (RECA-1), tumor cell proliferation (Ki-67), and tumor cell apoptosis (TUNEL).
*Significant. (n.s., not significant).

with MMCM has been successfully applied to generate sensitive noninvasive surrogate markers of tumor response to antiangiogenic therapy using different tumor–therapy combinations[28,29]. Consistent with our results, Raatschen et al.[29] reported a significant reduction of PS in experimental melanoma xenografts in rats as early as 24 h after a single application of the anti-VEGF antibody bevacizumab using DCE-MRI and the MMCM albumin-(Gd-DTPA)$_{35}$ with a molecular weight of 92 kDa. In their study, suppression of PS after 24 h, induced by a single dose of bevacizumab, correlated significantly with the observed change in tumor growth after a prolonged, multidose course of bevacizumab, leading them to conclude that functional parameters of tumor microcirculation may be applicable as sensitive biomarkers in cancer treatment monitoring[29]. Contrary to our current results, a previous DCE-MRI study with the clinically available SMCM gadobutrol (molecular weight 0.6 kDa) was not able to show significant effects of sorafenib on experimental prostate carcinomas on tumor endothelial permeability[5]. It was hypothesized that SMCM has reduced sensitivity for monitoring antiangiogenic therapy owing to the unselective, extracellular extravasation profile in physiologic and angiogenically overstimulated tissues alike. Conversely, MMCM with molecular weight

Table 3 **Assessment of tumor microcirculation with small molecular contrast media (SMCM)**

	PS		V_b		Blood flow	
	Correlation (r)	P value	Correlation (r)	P value	Correlation (r)	P value
RECA-1	0.38	n.s.	0.73	n.s.	0.56	0.01*
Ki-67	0.9	n.s.	0.48	n.s.	0.41	n.s.
TUNEL	0.82	n.s.	0.45	n.s.	−0.56	0.01*

Note the superior correlations observed with DCE-MRI parameters acquired with MMCM compared with data published previously in the same model with clinically available SMCM[7]. For SMCM, significant correlations were only observed for tumor plasma flow (ml/min/100 ml), a parameter not assessable with the Patlak model, used for kinetic analysis in the current MMCM study.
*Significant (n.s., not significant).

>60 kDa follow an intravascular distribution profile and do not readily extravasate across the tight endothelial barrier of physiologic vasculature. In tissues with elevated expression of VEGF, however, pronounced endothelial fenestrations and a leaky lamina basilaris allow for the extravasation of even larger proteins into interstitial space. In normal tissues with physiologic vasculature the expected PS is therefore close to zero, and any significant increase above zero is a sign of protein extravasation, which in tumor growth is predominantly influenced by VEGF/vascular permeability factor (VPF) expression[30]. The proportion of MMCM that extravasates (extraction fraction) is equal to that of protein and is thus variable in time. Since proteins extravasate slowly, the build-up of concentration in the extravascular space is slow, and a long measurement time is required to identify a clear trend. Preliminary measurements have shown that the uptake can be clearly resolved with a 1-h acquisition, and that no washout is visible[31]. Because of this specific extravasation profile, MMCM allow for the sensitive, noninvasive assessment of functional parameters such as tumor endothelial permeability and vascular richness in tissues with increased angiogenesis, as demonstrated in our study. Compared with the clinically available SMCM with molecular weight <1 kDa and an extracellular distribution profile, experimental MMCM such as albumin-$(Gd\text{-}DTPA)_{35}$ have been shown to be more sensitive in the assessment of angiogenic activity of tissues[15]. However, because of reduced bioelimination and concerns of potential immunogenicity, the MMCM prototype albumin-$(Gd\text{-}DTPA)_{35}$ is not suitable for human use. Alternative macromolecular MR contrast media are under development with the proclaimed aim of clinical translation[32,33]. The main obstacles toward the clinical introduction of macromolecular MR contrast media include high developmental costs and possible toxicity effects associated with poor or prolonged excretion of gadolinium.

Immunohistochemical correlation

Our study demonstrated significant correlations between PS, quantified by DCE-MRI and MMCM, and immunohistochemical assessments of tumor vascularity (RECA-1), tumor cell proliferation (Ki-67), and tumor cell apoptosis (TUNEL). V_b, as a parameter of tumor vascularity, correlated significantly with the immunohistochemical quantifications of tumor vascularity (RECA-1) and tumor cell proliferation (Ki-67). No significant correlation was observed between V_b and tumor cell apoptosis (TUNEL). A possible link between the noninvasively imaged endothelial permeability to macromolecules and angiogenic activity in tumor tissue is provided by the known dual actions of VEGF, also named VPF, as a potent modulator of angiogenic activity and endothelial permeability[28,34,35]. Compared with previous perfusion studies with SMCM in the same tumor/therapy combination (Table 2), superior correlations between MRI perfusion parameters and immunohistochemistry were achieved when imaging with MMCM[5,36]. Although not all parameters are comparable between the studies because of differences in kinetic analysis, Pearson's correlation coefficients approaching −0.9, as shown between MRI-assayed tumor endothelial permeability and tumor cell apoptosis, support an excellent noninvasive reflection of in vivo tumor biology when imaging with MMCM. As knowledge about the physiology of functional kinetic parameters reflecting different aspects of tumor biology progresses, DCE-MRI with MMCM may become a very reliable technique for monitoring therapy response of tumors to antiangiogenic therapy, pending clinical translation of macromolecular MRI contrast media.

Limitations

The results of our study are limited in several aspects. Prostate carcinomas were investigated as subcutaneous syngeneic tumor allografts in rats with possibly limited translational relevance for human tumor physiology. DCE-MRI studies were enhanced with albumin-$(Gd\text{-}DTPA)_{35}$, an MMCM not suitable for human use owing to concerns of bioelimination and immunogenicity. Until the possible advent of a clinically approved MMCM, further studies for the validation and standardization of DCE-MRI with clinically available, SMCM have to be performed, in full awareness of its methodological limitations. The Patlak model was chosen because tracer loss from interstitial space was assumed to be negligible within the acquisition time, and because

any dispersion in the vasculature would not be measureable with the very low temporal resolution of the acquired data. As a result, the interstitial volume and tissue blood flow could not be measured from these data, as this would have required a significantly higher temporal resolution, resulting in a loss of spatial resolution and coverage as well as acquisition times beyond 1 h, which was not practically feasible in this study. However, the validity of the model assumptions was verified in all data: The Patlak model provided a good fit to all measured ROI curves. In this study a 3D sequence with a low sampling rate was used. There may be room for data improvement by using a 2-dimensional sequence with a higher sampling rate or by selecting ROIs over several slices. Furthermore, immunohistochemical analysis represents only parts of the entire tumor. Apart from tissue quality, different staining protocols, and experimental settings, the results may be influenced by personal experience.

Conclusions

The results acquired by DCE-MRI with MMCM are in good correlation with the immunohistochemically assessed antiangiogenic, antiproliferative, and proapoptotic effects of a 1-week, daily treatment course of sorafenib on experimental prostate carcinoma allografts. This preclinical study provides evidence that in DCE-MRI, MMCM reflect tumor biology more reliably than clinically available SMCM. Pending clinical translation, MMCM perfusion parameters may serve as noninvasive imaging biomarkers of therapy response with superior noninvasive reflection of tumor biology in vivo.

Acknowledgements

Financial support for this project was provided by a research grant from Bayer Pharma AG, the Friedrich-Baur-Foundation, and the Foundation Foerderung fuer Forschung und Lehre of the Ludwig-Maximilians-University Munich.

Conflict of interest

The authors declare that they have no conflicts of interest.

References

[1] Cohen MH, Gootenberg J, Keegan P, Pazdur R. FDA drug approval summary: bevacizumab plus FOLFOX4 as second-line treatment of colorectal cancer. Oncologist 2007; 12: 356–361.

[2] Ferrara N, Gerber HP, LeCouter J. The biology of VEGF and its receptors. Nat Med 2003; 9: 669–676.

[3] Riedel F, Gotte K, Li M, Hormann K, Grandis JR. Abrogation of VEGF expression in human head and neck squamous cell carcinoma decreases angiogenic activity in vitro and in vivo. Int J Oncol 2003; 23: 577–583.

[4] Aragon-Ching JB, Jain L, Gulley JL, et al. Final analysis of a phase II trial using sorafenib for metastatic castration-resistant prostate cancer. BJU Int 2009; 103: 1636–1640.

[5] Cyran CC, Paprottka PM, Schwarz B, et al. Perfusion MRI for monitoring the effect of sorafenib on experimental prostate carcinoma: a validation study. AJR Am J Roentgenol 2012; 198: 384–391.

[6] Chang YS, Adnane J, Trail PA, et al. Sorafenib (BAY 43-9006) inhibits tumor growth and vascularization and induces tumor apoptosis and hypoxia in RCC xenograft models. Cancer Chemother Pharmacol 2007; 59: 561–574.

[7] Liu L, Cao Y, Chen C, et al. Sorafenib blocks the RAF/MEK/ERK pathway, inhibits tumor angiogenesis, and induces tumor cell apoptosis in hepatocellular carcinoma model PLC/PRF/5. Cancer Res 2006; 66: 11851–11858.

[8] Delgado JS, Mustafi R, Yee J, et al. Sorafenib triggers antiproliferative and pro-apoptotic signals in human esophageal adenocarcinoma cells. Dig Dis Sci 2008; 53: 3055–3064.

[9] Lam ET, Ringel MD, Kloos RT, et al. Phase II clinical trial of sorafenib in metastatic medullary thyroid cancer. J Clin Oncol 2010; 28: 2323–2330.

[10] Wahl RL, Jacene H, Kasamon Y, Lodge MA. From RECIST to PERCIST: evolving considerations for PET response criteria in solid tumors. J Nucl Med 2009; 50(Suppl 1): 122S–150S.

[11] Turetschek K, Preda A, Floyd E, et al. MRI monitoring of tumor response following angiogenesis inhibition in an experimental human breast cancer model. Eur J Nucl Med Mol Imaging 2003; 30: 448–455.

[12] De Visschere P, Oosterlinck W, De Meerleer G, Villeirs G. Clinical and imaging tools in the early diagnosis of prostate cancer, a review. JBR-BTR 2010; 93: 62–70.

[13] Miles KA. Molecular imaging with dynamic contrast-enhanced computed tomography. Clin Radiol 2010; 65: 549–556.

[14] Desar IM, Ter Voert EG, Hambrock T, et al. Functional MRI techniques demonstrate early vascular changes in renal cell cancer patients treated with sunitinib: a pilot study. Cancer Imaging 2012; 11: 259–265.

[15] Cheng HL, Wallis C, Shou Z, Farhat WA. Quantifying angiogenesis in VEGF-enhanced tissue-engineered bladder constructs by dynamic contrast-enhanced MRI using contrast agents of different molecular weights. J Magn Reson Imaging 2007; 25: 137–145.

[16] Cai W, Chen X. Multimodality molecular imaging of tumor angiogenesis. J Nucl Med 2008; 49(Suppl 2): 113S–128S.

[17] Coultas L, Chawengsaksophak K, Rossant J. Endothelial cells and VEGF in vascular development. Nature 2005; 438: 937–945.

[18] Preda A, van Vliet M, Krestin GP, Brasch RC, van Dijke CF. Magnetic resonance macromolecular agents for monitoring tumor microvessels and angiogenesis inhibition. Invest Radiol 2006; 41: 325–331.

[19] Ogan MD, Schmiedl U, Moseley ME, Grodd W, Paajanen H, Brasch RC. Albumin labeled with Gd-DTPA. An intravascular contrast-enhancing agent for magnetic resonance blood pool imaging: preparation and characterization. Invest Radiol 1987; 22: 665–671.

[20] Sourbron S, Dujardin M, Makkat S, Luypaert R. Pixel-by-pixel deconvolution of bolus-tracking data: optimization and implementation. Phys Med Biol 2007; 52: 429–447.

[21] Sourbron SP, Michaely HJ, Reiser MF, Schoenberg SO. MRI-measurement of perfusion and glomerular filtration in the human kidney with a separable compartment model. Invest Radiol 2008; 43: 40–48.

[22] Preda A, Turetschek K, Daldrup H, et al. The choice of region of interest measures in contrast-enhanced magnetic resonance image characterization of experimental breast tumors. Invest Radiol 2005; 40: 349–354.

[23] Brasch RC, Daldrup H, Shames D, Wendland M, Okuhata Y, Rosenau W. Macromolecular contrast media-enhanced MRI

estimates of microvascular permeability correlate with histopathologic tumor grade. Acad Radiol 1998; 5(Suppl 1): S2–S5.

[24] Bruns CJ, Harbison MT, Davis DW, et al. Epidermal growth factor receptor blockade with C225 plus gemcitabine results in regression of human pancreatic carcinoma growing orthotopically in nude mice by antiangiogenic mechanisms. Clin Cancer Res 2000; 6: 1936–1948.

[25] Hammerstingl R, Adam G, Ayuso JR, et al. Comparison of 1.0 M gadobutrol and 0.5 M gadopentetate dimeglumine-enhanced magnetic resonance imaging in five hundred seventy-two patients with known or suspected liver lesions: results of a multicenter, double-blind, interindividual, randomized clinical phase-III trial. Invest Radiol 2009; 44: 168–176.

[26] Turetschek K, Preda A, Novikov V, et al. Tumor microvascular changes in antiangiogenic treatment: assessment by magnetic resonance contrast media of different molecular weights. J Magn Reson Imaging 2004; 20: 138–144.

[27] Pradel C, Siauve N, Bruneteau G, et al. Reduced capillary perfusion and permeability in human tumour xenografts treated with the VEGF signalling inhibitor ZD4190: an in vivo assessment using dynamic MR imaging and macromolecular contrast media. Magn Reson Imaging 2003; 21: 845–851.

[28] Cyran CC, Sennino B, Chaopathomkul B, et al. Magnetic resonance imaging for monitoring the effects of thalidomide on experimental human breast cancers. Eur Radiol 2009; 19: 121–131.

[29] Raatschen HJ, Simon GH, Fu Y, et al. Vascular permeability during antiangiogenesis treatment: MR imaging assay results as biomarker for subsequent tumor growth in rats. Radiology 2008; 247: 391–399.

[30] Cyran CC, Sennino B, Fu Y, et al. Permeability to macromolecular contrast media quantified by dynamic MRI correlates with tumor tissue assays of vascular endothelial growth factor (VEGF). Eur J Radiol 2011; 81: 891–896.

[31] Roberts HC, Saeed M, Roberts TP, et al. Comparison of albumin-(Gd-DTPA)-30 and Gd-DTPA-24-cascade-polymer for measurements of normal and abnormal microvascular permeability. J Magn Reson Imaging 1997; 7: 331–338.

[32] Huang R, Han L, Li J, et al. Chlorotoxin-modified macromolecular contrast agent for MRI tumor diagnosis. Biomaterials 2011; 32: 5177–5186.

[33] Cyran CC, Fu Y, Raatschen HJ, et al. New macromolecular polymeric MRI contrast agents for application in the differentiation of cancer from benign soft tissues. J Magn Reson Imaging 2008; 27: 581–589.

[34] Dvorak HF, Nagy JA, Feng D, Brown LF, Dvorak AM. Vascular permeability factor/vascular endothelial growth factor and the significance of microvascular hyperpermeability in angiogenesis. Curr Top Microbiol Immunol 1999; 237: 97–132.

[35] Dvorak HF. Vascular permeability factor/vascular endothelial growth factor: a critical cytokine in tumor angiogenesis and a potential target for diagnosis and therapy. J Clin Oncol 2002; 20: 4368–4380.

[36] Cyran CC, von Einem JC, Paprottka PM, et al. Dynamic contrast-enhanced computed tomography imaging biomarkers correlated with immunohistochemistry for monitoring the effects of sorafenib on experimental prostate carcinomas. Invest Radiol 2012; 47: 49–57.